Proceedings of the ASME 2010 3rd Joint US-European Fluids Engineering Summer Meeting and 8th International Conference on Nanochannels, Microchannels, and Minichannels
FEDSM-ICNMM2010
August 1-5, 2010, Montreal, Canada

FEDSM-ICNMM2010-30353

THE DYNAMIC BEHAVIOR OF AN ADAPTIVE LIQUID MICROLENS DRIVEN BY A FERROFLUIDIC TRANSDUCER

Wenjia Xiao
Center of Smart Interfaces, Technische Universität Darmstadt, Petersenstr. 32, 64287 Darmstadt, Germany

Steffen Hardt
Center of Smart Interfaces, Technische Universität Darmstadt, Petersenstr. 32, 64287 Darmstadt, Germany

ABSTRACT

Ferrofluids are superparamagnetic suspensions of nanoparticles that can be used as transducers in microfluidic systems, among others. In corresponding setups a microscopic enclosure such as a microchannel is filled with a ferrofluid that is acted on by an external magnetic field. The induced motion of the ferrofluid is utilized to pump or manipulate minute amounts of liquids. Here the dynamic behavior of an adaptive liquid microlens driven by a ferrofluidic transducer is studied. Adaptive microlenses based on that principle promise a number of advantages over existing concepts, such as an increased tuning range of the focal length. It is shown that the delay time of the deformation of the lens surface to the displacement of the magnet producing the external field increases with increasing magnet speed. Dynamic leakage of the lens liquid around the ferrofluid plug, on the other hand, only occurs when the magnet speed exceeds a threshold value and further increases from that point onwards. When the viscosity of the lens liquid increases, both the delay time and the dynamic leakage increase.

1. INTRODUCTION

Adaptive lenses can change their focal length without moving parts and therefore are particularly attractive for miniaturized optical systems [1-5]. Liquids have been long known to be suitable for such adaptive lenses due to their ability to form extremely smooth and spherical surfaces [2-3]. Compared to adaptive lenses using liquid crystals whose refractive indices change with the applied electric field, liquid lenses are capable of seamlessly switching from concave to convex shapes and thus provide relatively large changes of the focal length [6-10]. The standard way to obtain adaptive liquid lenses has been based on electrowetting where the curvature of the interface between two immiscible liquids can be controlled by applying an electrostatic potential [11-15]. However, eliminating the “stick-slip behavior” originating from contact angle (CA) hysteresis remains a challenge for electrowetting lenses [13, 15]. Moreover, electrowetting lenses require a relatively high voltage (of the order of 100 V) that limits their application in portable systems [13, 14], and their tuning range is limited because of contact-angle saturation [12]. An alternative principle is based on stimuli-responsive hydrogels that are able to change the curvature of a liquid lens by volumetric changes of the surrounding wall material [2]. While such an approach is surely attractive due to the large achievable tuning range for the focus, it is limited through the slow response times of the hydrogel that result in switching times of some ten seconds.

We recently presented an adaptive liquid microlens driven by a ferrofluidic transducer, opening the door to much lower driving voltages than required for electrowetting lenses [16]. The microlens is reversibly tunable without hysteresis within a large range of operation parameters and provides a relatively large tuning range of the focal length compared to liquid crystal and electrowetting lenses [11-15]. Moreover, owing to the comparatively fast response of the ferrofluid to changes in the magnetic field, the described principle is suited for fast switching processes. In this paper, the dynamic behavior of the liquid microlens is studied by analyzing the delay between the deformation of the liquid surface and the displacement of a permanent magnet producing the external field. The dependence of the dynamic leakage of the lens liquid around the ferrofluid plug on the magnet speed is also investigated.

2. CONCEPT OF THE FERROFLUIDIC TRANSDUCER

Ferrofluids are stable colloidal suspensions of ferromagnetic nanoparticles (with a typical size of 10 nm) in aqueous or organic carriers. In the absence of a magnetic field, the nanoparticles are randomly oriented, thus ferrofluids have no net permanent magnetization. Conversely, when a magnetic field is applied to a ferrofluid, the nanoparticles tend to stay aligned with the direction of the orienting field. Assume that the nanoparticles are noninteracting thermally agitated magnetic dipoles. The magnetization M of a ferrofluid volume as a function of the applied magnetic field H can be described using the Langevin function [17]:

$$M = nm\left(coth\alpha - \frac{1}{\alpha}\right), \tag{1}$$

$$\alpha = \frac{mH}{kT}, \tag{2}$$

where n, k, and T is the number density of nanoparticles, Boltzmann constant, and temperature, respectively. The magnetic moment of a single nanoparticle is given by $m = \pi d^3 \mu_0 M_b/6$, containing the particle size d, the free-space permeability μ_0, and the saturation magnetization M_b of the bulk magnetic material. We can see that, under weak magnetic fields, the tendency of the nanoparticles to stay aligned with the applied field is partially overcome by the thermal agitation. As the field strength increases, the nanoparticles become more and more aligned with the field direction. At very high field strengths the nanoparticles become completely aligned, and the magnetization achieves its saturation value. The magnetization of a ferrofluid responds quickly to any change in the applied magnetic field and the moments randomize rapidly when the applied field is removed. The moments can randomize through two distinct mechanisms: particle rotation with a time constant $\tau_B = \pi d^3\eta/2kT$, where η is the viscosity of the carrier, and rotation of the magnetic vectors that happens within $\tau_N = exp\ (\pi d^3 K/6kT)/f$ under the condition that $KV \ll kT$, where $f \approx 109$ Hz, K is the anisotropy constant, and V the particle volume. Particle rotation occurs in the case $\tau_B \ll \tau_N$, while magnetic vector rotation dominates if $\tau_N \ll \tau_B$. Water-based ferrofluids usually randomize through particle rotation with τ_B being less than 100 µs due to their relatively large particles compared to those in organic carriers. This suggests that ferrofluids can be regarded as superparamagnetic for general technical applications where the time scale is much greater than τ_N or τ_B.

The net force per unit ferrofluid volume F_m subjected to an external magnetic field H corresponding to a magnetic stress tensor T_m can be expressed by [17]

$$F_m = -\boldsymbol{\nabla} \cdot T_m = M\boldsymbol{\nabla} H. \tag{3}$$

The ferrofluid responds as a homogeneous magnetic liquid, and since the force on a ferrofluid volume is proportional to the gradient of the applied magnetic field $\boldsymbol{\nabla} H$, it moves to the region of highest magnetic field strength. This means that a ferrofluid volume can be precisely positioned and dynamically controlled by applying an external magnetic field. According to the Navier-Stokes equation, the motion of a ferrofluid is given by [17]

$$\rho \frac{Dv}{Dt} = -\boldsymbol{\nabla} P + \eta \boldsymbol{\nabla}^2 v + M\boldsymbol{\nabla} H, \tag{4}$$

where ρ, v, P, and η is the density, velocity, pressure, and dynamic viscosity, respectively. Since, according to equation (1), M saturates for sufficiently high values of the magnetic field strength, in that case the magnetic force density is simply proportional to $\boldsymbol{\nabla} H$.

The concept of the adaptive liquid microlens driven by a ferrofluidic transducer is illustrated by figure 1. A ferrofluid plug is moved back and forth inside a microchannel by applying an external magnetic field. The displacement of the ferrofluid plug translates to the displacement of a second immiscible liquid, comprising a liquid lens with an adaptive focus in a cylindrical well connected to the microchannel. Ultimately, the idea is to utilize microcoil arrays [18] to manipulate a ferrofluid plug in a microchannel. Temporarily, the action of the microcoil array was mimicked by attaching a permanent magnet with a suitable surface field to a linear motor.

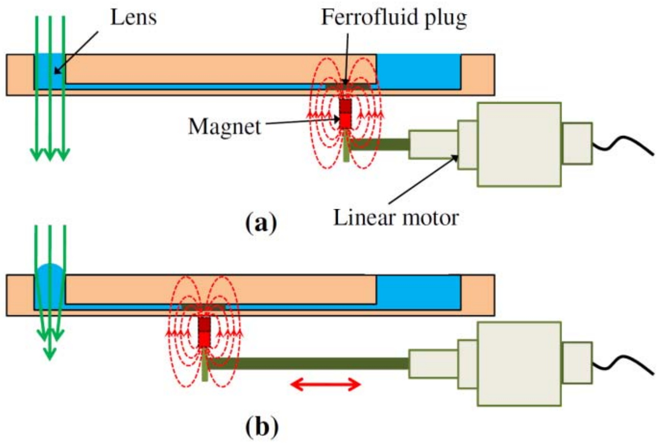

Fig. 1 Schematic cross section of the adaptive liquid microlens driven by a ferrofluidic transducer without (a) and with (b) convex surface profile. The lens liquid is displaced in the microchannel by a ferrofluid plug formed from a second immiscible liquid.

3. EXPERIMENTAL DETAILS

Figure 2 shows the experimental setup mainly comprising a metallic frame, a linear motor (NA08B16, Zaber Technologies Inc., Canada), a microfluidic chip, and a permanent magnet (Gaussboys Super Magnets, Portland, OR) with a size of 1.5 mm × 1.5 mm × 0.75 mm and a surface field of about 140 mT. Both the linear motor and the microfluidic chip are mounted to the frame. The magnet is attached to the thrust rod of the linear motor and can be moved back and forth under the microfluidic chip. The distance between the channel and the magnet is about 150 µm. The speed and displacement of the magnet can be controlled by the linear motor with the help of an installed Zaber Console software. The experimental setup is built on the sample stage of a CA measurement instrument (DSA100, Krüss GmbH, Germany). The lens profile and thus the intersection angle (IA) between the liquid microlens and the chip surface can be measured by the CA measurement instrument with the help of an installed drop shape analysis software. The CA measurement is also employed to check the delay of the lens to the magnet by recording videos with a frame rate of 25 frames per second.

The microfluidic chip is made of polymethylmethacrylate (PMMA) and mainly consists of two cylindrical wells being about 26 mm apart from center to center connected to each other at the bottom by a rectangular microchannel of about 1.0 mm in width and 170 µm in depth, as illustrated by figure 3. The smaller well is 2 mm in diameter and used for the lens housing, while the bigger one serves as a liquid reservoir and has a diameter of 5 mm. To fabricate the chip, a PMMA substrate (50 mm × 30 mm × 3 mm) is first patterned by conventional mechanical milling with two cylindrical through holes connected by a rectangular groove. To form the microfluidic chip, the patterned chip is then covered with a PMMA foil of 125 µm in thickness via solvent bonding with isoamyl acetate, applying a pressure of 42 kPa over a period of 5 min. All surfaces of the chip are finally chemically modified by rinsing them with a commercial antispread liquid (TE1403DA53, Dr. Tillwich GmbH, Germany).

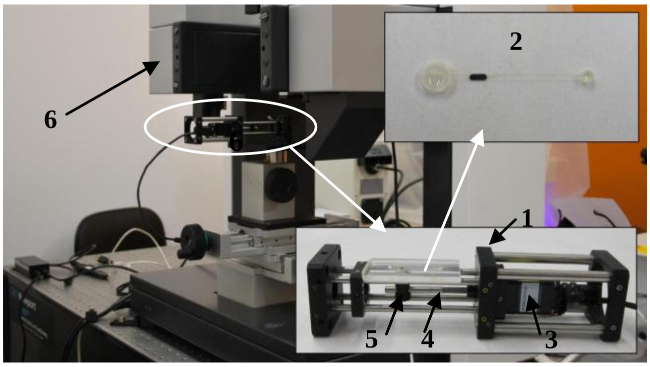

Fig. 2 Photograph of the experimental setup with a top view of the microfluidic chip in the inset. 1 - metallic frame, 2 - microfluidic chip, 3 – linear motor, 4 – thrust rod of linear motor, 5 – saddle for holding the magnet, and 6 - CA measurement instrument.

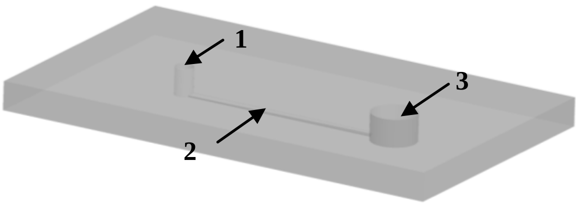

Fig. 3 Schematic of the microfluidic chip. 1 - cylindrical housing for liquid lens, 2 - microchannel, and 3 - liquid reservoir.

A water-based ferrofluid (EMG705, Ferrotec Corp., USA) is used as the transducer, characterized by a density, volume fraction of Fe3O4, average particle diameter, viscosity, and saturation field of 1.19 g/cm^3 at 25 ℃, 3.6%, 10 nm, 5 mPa·s at 27 ℃, and 20 mT, respectively. A mixture of hydrogenated terphenyl and 1-bromonaphthalene (No. 18095, Cargille Labs, USA), which is immiscible with the ferrofluid, is used as lens liquid. The density, viscosity, and surface tension of the liquid is 1.385 g cm^{-3}, 11 mPa·s, and 410 µN cm^{-1} at 25℃, respectively.

The lens liquid is injected through a Teflon tube fitted to the cylindrical well using a syringe. After the wells and the microchannel are almost completely filled with lens liquid, a small portion of ferrofluid is dropped into the liquid reservoir and guided into the channel by the magnetic field. The amount of ferrofluid injection is carefully controlled so that the ferrofluid plug inside the microchannel is about 2.5 mm in length.

4. RESULTS AND DISCUSSION

4.1 Theoretical description

To suppress gravitational impacts on the shape of the liquid lens, the base radius of the microlens should be smaller than the capillary length of the lens liquid (which is $k^{-1} = \sqrt{\gamma/\rho g}$, where γ is the surface tension, g is the gravitational acceleration and ρ the liquid density) [19]. In that case, the lens approximately takes on the shape of a spherical cap in accordance with Laplace's equation. Assume that the leakage of the lens liquid around the ferrofluid plug is negligible. The relationship between the radius of the lens surface r and the ferrofluid displacement D can be expressed from mass conservation:

$$\frac{D}{R} = \frac{\pi R^2}{3A}\left(\frac{2-3cos\theta+cos^3\theta}{sin^3\theta}\right) \tag{5}$$

$$\frac{r}{R} = \frac{1}{sin\,\theta} \tag{6}$$

where $A = ab$ is the cross sectional area of the channel, θ the IA between the liquid lens and the chip surface, and R the base radius of lens. Figure 4 shows the relationship between D/R and r/R for different A/R^2 values. We can see that the relationship between D/R and r/R can be controlled by modifying A/R^2. For a lens with fixed base radius, D decreases with increasing A/R^2.

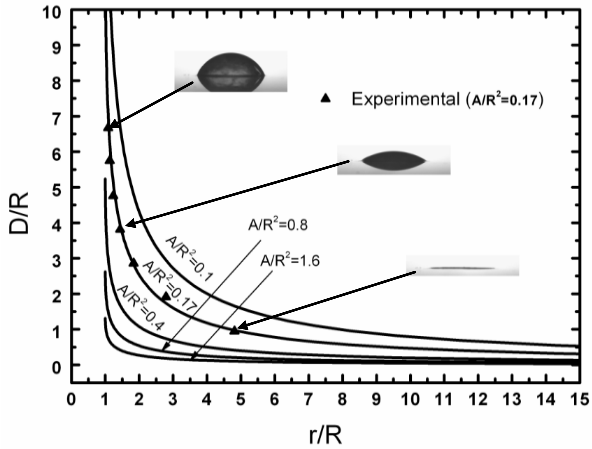

Fig. 4 The ferrofluid displacement D normalized by R as a function of the radius of curvature of the lens surface r normalized by R for different A/R^2 values. Symbols show the measurements where D was obtained from the displacement of the magnet. The insets are corresponding photographs of the lens profile.

Assuming that the ferrofluid plug follows the magnet without delay, on the other hand, the switching time $t_{1,2}$ between two lens states (i.e. $\theta = \theta_1$ and $\theta = \theta_2$) is given by

$$t_{1,2} = \frac{\pi R^3}{3A\dot{D}}\left[\frac{2-3cos\theta+cos^3\theta}{sin^3\theta}\right]\Big|_{\theta_1}^{\theta_2} \tag{7}$$

where $\dot{D}$ is the speed of the magnet and $[\cdot]|_{\theta_1}^{\theta_2}$ denotes the subtraction between the values of the function $[\cdot]$ at $\theta = \theta_1$ and $\theta = \theta_2$. We can see that for a lens with fixed base radius, $t_{1,2}$ can be reduced by increasing either the cross sectional area of the channel or the magnet speed. For the device presented here, it would require about 940 milliseconds to switch the IA from 0º to 30º in the case of $\dot{D}$ = 2.7 mm/s, which results in a focal length change from infinity to about 3.1 mm. On the other hand, $t_{1,2}$ decreases as the third power of the base radius of the lens, which means that a reduction of the base radius leads to a dramatic decrease of $t_{1,2}$. Once the speed of the magnet exceeds a threshold value, however, the ferrofluid plug cannot follow the trajectory of the moving magnetic field anymore. This threshold value results from a balance of the friction force F_φ, the maximum magnetic force F_m, and the Laplace pressure force F_L originating from the curved liquid surfaces in the two cylindrical wells, i.e.

$$F_\varphi + F_m + F_L = 0. \tag{8}$$

A simple order-of-magnitude estimate shows that the Laplace pressure force is much smaller than the maximum magnetic force, so it will not be considered in the following. For a rectangular channel, the friction force is approximately given by [20]

$$F_\varphi = \frac{dP}{dx}AL = -\frac{2\rho u^2}{D_h}\varphi AL \tag{9}$$

$$\varphi = \frac{24}{Re}(1 - 1.3553\alpha + 1.9467\alpha^2 - 1.7012\alpha^3 + 0.9564\alpha^4 - 0.2537\alpha^5) \tag{10}$$

where α is the aspect ratio of the channel (i.e. b/a), L its length, and D_h the hydraulic diameter given by $2ab/(a+b)$. The Reynolds number is given by $Re = D_h\rho u/\eta$, containing the average flow speed u and the density and viscosity of the liquid, ρ and η.

The above analysis does not consider the dynamic leakage of the lens liquid around the ferrofluid plug that occurs at high magnet speeds. Once the dynamic leakage occurs, the focal length can no longer be adjusted in a reversible manner. Therefore, a further requirement is that the magnet should be moved at a speed lower than the threshold where dynamic leakage occurs. On the other hand, the above discussion suggests that equation (7) is not expected to give an accurate description of the switching dynamics when either the ferrofluid plug lags behind the magnet or dynamic leakage occurs.

4.2 Experimental results

The ferrofluid is moved inside the microchannel by the magnet, leaving no observable trace behind. The relationship between the magnet displacement D normalized by R and r normalized by R as obtained from experiments with $\dot{D}$ = 1.8 mm/s is plotted in figure 4. Due to the fact that R =1 mm is less than k^{-1} =1.76 mm for the lens liquid used, the lens is treated as spherical cap and thus r/R is calculated according to equation (6). We can see that the experimental data fit the theoretical prediction well, indicating that the ferrofluid plug follows the external magnetic field without any significant bypass flow of lens liquid around the ferrofluid plug. The focal length of the liquid lens f can be estimated based on $f = r/n - 1 = R/(n-1)/sin\theta$, where n is the refractive index of the lens liquid. The experimental range of magnet displacement from 0 to 6.67 mm corresponds to a tuning range of the focal length between 1.7 mm and infinity. The chosen principle allows to change the focal length of the microlens from infinity to the scale of its base radius (that could be of the order of 100 µm if desired), promising a great optical power compared to conventional liquid lenses.

The liquid microlens is reversibly tunable without observed hysteresis which ubiquitously exists in electrowetting lenses [15] when the magnet moves at a speed below a threshold value, as indicated by figure 5. The threshold value depends on the properties of the lens liquid. Once the magnet speed exceeds a certain threshold, however, the reversibility of lens adaption cannot be achieved anymore, an effect that is probably due to the dynamic leakage of the lens liquid around the ferrofluid plug. As shown in figure 5, both the lower IA and upper IA of the lens increase gradually with an increasing number of cycles at a magnet speed of 3.6 mm/s, indicating an obvious bypass flow of the lens liquid around the ferrofluid plug. The dynamic leakage becomes more obvious as the magnet speed increases further to 5.4 mm/s. In that case, the lower IA increases from 24.3º to 34.6º while the upper IA increases from 51.3º to 60.6º after 10 cycles.

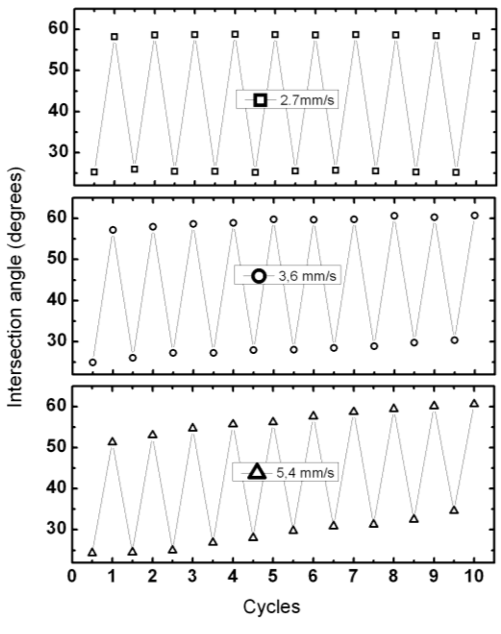

Fig. 5 Evolution of the IA between the liquid lens and chip surface during successive cycles of switching between two different states. The speed of the magnet is 2.7 mm s^{-1}, 3.6 mm s^{-1}, and 5.4 mm s^{-1}, respectively (from top to bottom), its displacement 3.8 mm in each case.

Figure 6 shows the interface between the ferrofluid and lens liquid inside the microchannel without magnetic field. The contact angle of the ferrofluid on the channel wall is estimated to be $\theta_s = 167$º. When the ferrofluid moves to the right, however, the contact angle will increase, assuming a value of

θ_d. This dynamic contact angle depends on the capillary number of the lens liquid $Ca = \eta v/\gamma$ where η, v and γ denote the dynamic viscosity of the lens liquid, the flow speed and the interfacial tension, respectively, and is given by [21]

$$\theta_d \approx \theta_s + \beta Ca^{1/3} \tag{11}$$

where β is a constant. As a result of equation (11), once the ferrofluid plug moves with a sufficiently high speed, θ_d could reach the limiting value of 180º. In that case, a liquid film forms between the ferrofluid and the channel wall, enabling a bypass flow of lens liquid around the plug. This effect could explain the dynamic leakage that only occurs if the magnet speed exceeds a certain threshold value.

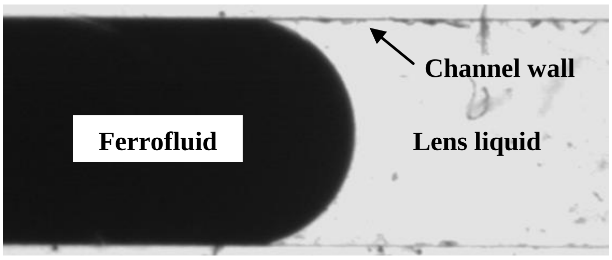

Fig. 6 Photograph of the interface between the ferrofluid and lens liquid inside the channel without magnetic field. The contact angle of the ferrofluid on the channel wall is about 167º.

Due to the fact that the length of the ferrofluid plug (i.e. about 2.5 mm) is relatively small compared to the length of channel (i.e. about 22.5 mm) in the experiment, the friction force mainly comes from the lens liquid. According to equations (9) and (10), we get F_f = 1.97 × 10^{-2} N·s·m^{-1} u. Based on equations (1) and (2) with M_b being about 4.5 × 10^5 Am^{-1} for Fe_3O_4 [17], on the other hand, the magnetic moment of the ferrofluid plug μ_f is about 5.7 × 10^{-6} A·m^{-1} and thus the magnetic force is $F_m = \mu_f \boldsymbol{\nabla} H$ = 5.7 × 10^{-6} N·m·T^{-1} **∇**H. Assuming that $\boldsymbol{\nabla} H$ = 100 mT/mm which is the order of magnitude of the magnetic field gradient provided by the permanent magnet, we get u = 13 mm/s. In our experiment, the ferrofluid plug can still follow the trajectory of the magnet even it moves at a maximum speed of 11.4 mm/s which is higher than the threshold value where dynamic leakage occurs. The above results indicate that in the case considered, a bypass flow occurs around the ferrofluid plug well before it is no longer able to follow the trajectory of the permanent magnet owing to viscous forces exceeding the magnetic forces. It suggests that the threshold speed where dynamic leakage begins to set in represents an orientation mark for the speed at which the magnet can be moved without compromising the reversibility of lens adaption.

To investigate the impact of viscosity of the lens liquid on the dynamic leakage, the lens has been studied after replacing the lens liquid by another liquid (Cannon calibration liquid) with a high viscosity of about 120 mPa·s at 23 °C. The evolution of the IA during successive cycles of switching between two different states is plotted in figure 7. We can see that the threshold value of the magnet speed where dynamic leakage occurs decreases when the viscosity of the lens liquid increases. There is an obvious dynamic leakage of the lens liquid around the ferrofluid plug when the magnet moves at a speed of 1.8 mm s^{-1} in the case of Cannon liquid, as indicated by figure 7. In the case of $\dot{D}$ = 2.7 mm s^{-1}, the lower IA increases from about 14.9º to about 36.8º while the upper IA increases from about 49.1º to about 63.0º after 8 cycles.

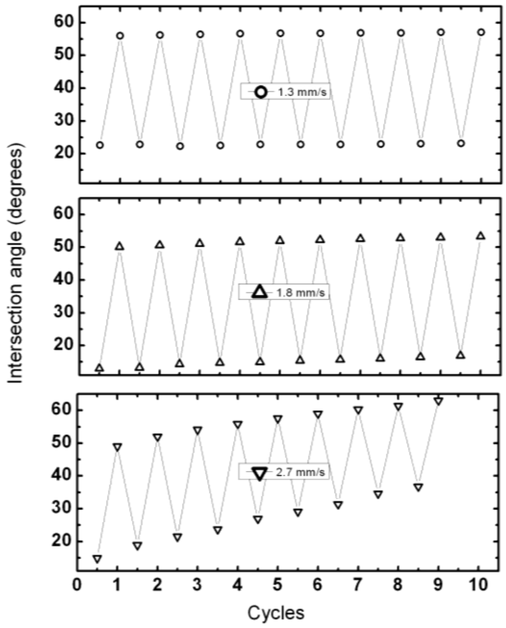

Fig. 7 Evolution of the IA between the liquid lens and chip surface during successive cycles of switching between two different states when Cannon liquid used as lens liquid. The speed of the magnet is 1.3 mm/s, 1.8 mm/s, and 2.7 mm/s, respectively (from top to bottom), its displacement 3.8 mm in each case.

The delay between the magnet and the deflection of the lens surface can be attributed to both the relative displacement between the magnet and ferrofluid plug and the deformation of the ferrofluid plug shape during the movement. The ferrofluid plug initially centers itself above the magnet in the channel and the net magnetic force acting on it is close to zero. A net magnetic force appears when a relative replacement between the magnet and ferrofluid plug occurs and reaches a maximum value when one end of the ferrofluid plug is at the center of the magnet. When the magnet moves at a certain speed, therefore, the position of the ferrofluid plug relative to the magnet shifts so that the net magnetic force acting on the ferrofluid plug is equal to the friction force caused by the movement. As indicated by equations (9), the friction force increases when the speed of the ferrofluid plug increases, leading to a greater relative displacement between the ferrofluid plug and magnet. At the same time, the ferrofluid plug is expected to deform during its movement, while the deformation increases with increasing flow speed. The increase of the delay time with increasing magnet speed in figure 8 could be explained by the fact that the larger the relative displacement and/or the deformation of the ferrofluid plug are, the longer it takes for the ferrofluid plug to change back to its initial position relative to the magnet and/or initial shape. Similarly, as indicated by equations (9) and (10), the friction force increases when the viscosity of lens liquid increases, resulting in a larger displacement between the magnet and the ferrofluid and a larger deformation of the ferrofluid plug. Therefore, an increase in viscosity should have the same effect as an augmentation of the magnet speed.

The scale of the delay time shown in figure 8, reaching a minimum value of about 80 ms, indicates that the observed dynamics is governed by fluid transport rather than magnetization dynamics of the ferrofluid. In section 2 the particle rotation time scale $\tau_B$was estimated to be of the order of 100 µs, much smaller than the time scales introduced through the relative displacement between the magnet and the ferrofluid plug in combination with the deformation of the latter.

Videos with a frame rate of 25 frames per second have been recorded to characterize the delay between the magnet and the deflection of the lens surface. The delay time is defined as the time during which the IA of the lens becomes stable after the magnet stops. The delay time increases with increasing magnet speed or increasing viscosity of lens liquid, as indicated by figure 8. In the case of Cargille liquid used as lens liquid, the delay time is about 80 ms at $\dot{D}$ = 0.9 mm s^{-1}, while it is about 200 ms at $\dot{D}$ = 2.7 mm s^{-1}. For the Cannon liquid, on the other hand, the delay time increases from about 80 ms to 1.8 s in the case of $\dot{D}$ = 0.9 mm s^{-1} while it increases from about 200 ms to 2.7 s for $\dot{D}$ = 2.7 mm s^{-1}, as indicated by figure 8.

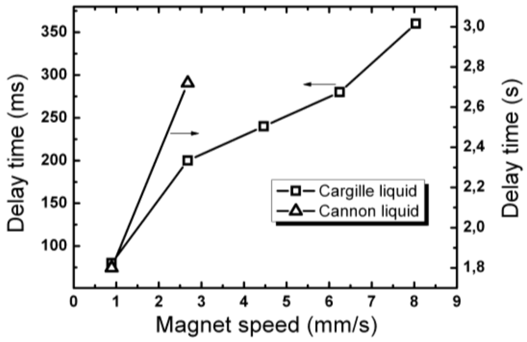

Fig. 8 The delay time between the liquid lens surface deflection and the magnet displacement for different magnet speeds. Square and triangle symbols represent the Cargille liquid and the Cannon liquid used as lens liquid, respectively.

5. CONCLUSIONS AND OUTLOOK

In conclusion, the use of ferrofluidic transducers in an optofluidic system, an adaptive liquid microlens, has been demonstrated, and the dynamic response to changes in the external magnetic field has been studied. The delay time increases from a few tens of milliseconds to several hundred milliseconds as the magnet speed increases from 0.9 mm/s to 8 mm/s when a lens liquid with a kinematic viscosity of 11 mPa·s is used. Dynamic leakage, most probably a bypass flow of lens liquid around the ferrofluid plug, only occurs when the speed exceeds a threshold value and further increases from that point onwards. Moreover, both the delay time and the dynamic leakage increase when the viscosity of the lens liquid increases. The delay time is most probably due to the relative displacement between the external magnet and the ferrofluid plug as well as the dynamic deformation of the latter. The results show that the principle of optofluidic components driven by ferrofluidic transducers allows a fast adaption of optical properties on the scale of some ten milliseconds. In the future, a microcoil array will be developed to drive the ferrofluid, thereby constituting a compact actuator without moving parts. Furthermore, the fluidic configuration of the system will be modified to reduce the intrinsic time scales and the bypass flow.

ACKNOWLEDGEMENT

Financial support from German Research Foundation under grant no. HA 2696/17-1 is gratefully acknowledged.

REFERENCES

[1] López, C. A., and Hirsa, A. H., 2008, "Fast focusing using a pinned-contact oscillating liquid lens," Nature Photon., 2, pp. 610-613.

[2] Dong, L., Agarwal, A. K., Beebe, D. J., and Jiang, H., 2006, "Adaptive liquid microlenses activated by stimuli-responsive hydrogels," Nature, 442, pp. 551-513.

[3] Ren, H., and Wu, S. T., 2005, "Variable-focus lens by changing aperture," Appl. Phys. Lett. 86, pp. 211107(1-3).

[4] Zhang, D. Y., Lien, V., Berdichevsky, Y., Choi, J., and Lo, Y, H., 2003, "Fluidic adaptive lens with focal length tunability," Appl. Phys. Lett., 82, pp. 3171-3172.

[5] Chen, J. C., Wang, W., Fang, J., and Varahramya, K., 2004, "Variable-focusing microlens with microfluidic chip," J. Micromech. Microeng., 14, pp. 675-680.

[6] Sato, S., 1979, "Liquid-crystal lens-cells with variable focal length," Jpn. J. Appl. Phys., 18, pp. 1679-1684.

[7] Patel, J. S., and Rastani K, 1991, "Electrically controlled polarization-independent liquid-crystal Fresnel lens arrays," Opt. Lett., 16, pp. 532-4.

[8] Ren, H., Fan, Y. H., Gauza, S., and Wu, S. T., 2003, "Tunable electronic lens using a gradient polymer network liquid crystal," Appl. Phys. Lett., 82, pp. 22-24.

[9] Ren, H., Fan, Y. H., Gauza, S., and Wu, S. T., 2004, "Tunable-focal flat-liquid crystal spherical lens," Appl. Phys. Lett., 84, pp. 4789-4791.

[10] Ye, M., Wang, B., and Sato, S., 2008, "Realization of liquid crystal lens of large aperture and low driving voltages using thin layer of weakly conductive material," Opt. Express, 16, pp. 4302-4308.

[11] Gorman, C. B., Biebuyck, H. A., and Whitesides, G. M., 1995, "Control of the shape of liquid lenses on a modified gold surface using an applied electrical potential across a self-assembled monolayer," Langmuir, 11, pp. 2242-6.

[12] Mugele, F., and Baret, J. C., 2005, "Electrowetting: from basis to applications," J. Phys.: Condens. Matter, 17, pp. R705-74.

[13] Krupenkin, T., Yang, S., and Mach, P., 2003, "Tunable liquid microlens," Appl. Phys. Lett., 82, pp. 316-318.

[14] Kuiper, S., and Hendriks, B. H. W., 2004, "Variable-focus liquid lens for miniature cameras," Appl. Phys. Lett., 85, pp. 1128-1130.

[15] Maillard, M., Legrand, J., and Berge, B., 2009, "Two liquids wetting and low hysteresis electrowetting on dielectric applications," Langmuir, 25, pp. (11) 6162-7.

[16] Xiao, W., and Hardt, S., 2010, "An adaptive liquid microlens driven by a ferrofluidic transducer," J. Micromech. Microeng., 20, pp. 055032(1-8).

[17] Rosensweig, R. E., 1985, Ferrohydrodynamics, Cambridge University Press, New York.
[18] Ruffert, C., and Gatzen, H. H., 2008, "Fabrication and test of multilayer microcoils with a high packaging density," Microsyst. Technol., 14, pp. 1589-1592.
[19] de Gennes, P. G., Brochard-Wyart, F., and Quéré, D., 2002, Capillarity and wetting phenomena-drops, bubbles, pearls, waves, Springer, New York, pp. 33-36.
[20] Shah, R. K., and London, A. L., 1978, "Laminar flow forced convection in ducts," Adv. Heat Transfer, Suppl. 1.
[21] Hoffman, R. L., 1975, "A study of the advancing interfaces. I. Interface shape in liquid-gas system," J. Colloid Interface Sci., 50, pp. 228-241.